Voltage-Clamp Studies of Gap Junctions Between Uterine Muscle Cells During Term and Preterm Labor

Hiroshi Miyoshi, Mary B. Boyle, Lynette B. MacKay, and Robert E. Garfield
Reproductive Sciences, Department of Obstetrics and Gynecology, University of Texas Medical Branch, Galveston, Texas 77555-1062 USA

ABSTRACT Gap junctions between myometrial cells increase dramatically during the final stages of pregnancy. To study the functional consequences, we have applied the double-whole-cell voltage-clamp technique to freshly isolated pairs of cells from rat circular and longitudinal myometrium. Junctional conductance was greater between circular muscle-cell pairs from rats delivering either at term (32 ± 16 nS, mean ± SD, n = 128) or preterm (26 ± 17 nS, n = 33) compared with normal preterm (4.7 ± 7.6 nS, n = 114) and postpartum (6.5 ± 10 nS, n = 16); cell pairs from the longitudinal layer showed similar differences. The macroscopic gap junction currents decayed slowly from an instantaneous, constant-conductance level to a steady-state level described by quasisymmetrical Boltzmann functions of transjunctional voltage. In half of circular-layer cell pairs, the voltage dependence of myometrial gap junction conductance is more apparent at smaller transjunctional voltages (<30 mV) than for other tissues expressing mainly connexin-43. This unusual degree of voltage dependence, although slow, operates over time intervals that are physiologically relevant for uterine muscle. Using weakly coupled pairs, we observed two unitary conductance states: 85 pS (85–90% of events) and 25 pS. These measurements of junctional conductance support the hypothesis that heightened electrical coupling between the smooth muscle cells of the uterine wall emerges late in pregnancy, in preparation for the massive, coordinate contractions of labor.

INTRODUCTION

Gap junctions between myometrial cells increase over 200-fold during the last 12 h of pregnancy in the rat, in both number and size (Garfield et al., 1977). The establishment of the junctions is thought to be one of the major steps toward labor, whereas their suppression before term is believed to help maintain uterine quiescence. Because electrical coupling between the billions of tiny smooth muscle cells is essential for coordinated labor, studies of gap junctional coupling and its regulation may provide important clues about the prevention of premature birth, the most critical problem in obstetrics.

The structural evidence for the increased expression gap junctions in parturition is compelling, based on extensive studies in both humans and animals. The increased incidence of gap junctions between myometrial cells of term and preterm delivering animals was first shown by electron microscopy (Garfield et al., 1978, 1982). Probes for connexin-43, the main connexin expressed in myometrium, have been used in demonstrating the induction of gap junction mRNA and protein in myometrium before labor begins (Risek et al., 1990; Lang et al., 1991; Hendrix et al., 1992; Tabb et al., 1992; Sakai et al., 1992a; Petrocelli and Lye, 1993).

Functional studies to this point have relied on indirect methods and have been used mainly to verify the predictions of increased electrical coupling. The induction of gap junctions late in pregnancy coincides with an enhancement in the propagation of action potential activity through the muscle, and electrophysiological studies have shown decreases in both junctional resistance and input resistance (Sims et al., 1982; Miller et al., 1989; Sakai et al., 1992b). The resolution of such studies is limited, however, because the facilitation of activity could reflect contributions from changes in plasma membrane currents, not only junctional conductance increases. The apparent diffusion coefficients of both 2-[^{3}H]deoxy-D-glucose and lucifer yellow are greater in human and rat myometrium at delivery than before or after parturition (Cole et al., 1985; Sakai et al., 1992b), as expected with stronger coupling.

More difficult questions about the functional consequences of the increases in gap junctions remain unanswered. It is not known whether the gap junction channels, once induced, are available for opening at all times or whether the precise timing of labor dictates a tighter control. The gating of gap junction channels can be modified by a number of second-messenger-mediated pathways. For example, in the myometrium, although not in cardiac muscle, the coupling between cells seems to be reduced acutely by cAMP (Cole and Garfield, 1986; Sakai et al., 1992b). Prolonged elevations of intracellular calcium such as occur during a labor contraction may also have the potential to affect gap junctions (e.g., channel closure, as in heart; Noma and Tsuboi, 1987). To address these issues requires a preparation in which cellular mechanisms can be studied.

The double-whole-cell voltage-clamp method, which allows simultaneous intracellular recording from each cell in an isolated pair of cells, permits questions about the electrical pathways between cells to be asked more rigorously

Received for publication 6 November 1995 and in final form 3 June 1996.
Address reprint requests to Dr. Robert E. Garfield, Reproductive Sciences, Department of Obstetrics and Gynecology, University of Texas Medical Branch, 11.102 MRB, 301 University Blvd., Galveston, TX 77555-1062. Tel.: 409-772-7590; Fax: 409-772-2261; E-mail: robert.garfield@utmb.edu.

0006-3495/96/09/1324/11 $2.00

(Neyton and Trautmann, 1985; White et al., 1985). In the present experiments, the double voltage-clamp method was applied to pairs of cells from uterine muscle for the first time. Pairs of smooth muscle cells were freshly isolated from the myometrium of pregnant rat uterus during late pregnancy (days 16 and 19), during RU-486-induced preterm delivery (on day 19), at term just before delivery and during delivery (day 22), and 1 day postpartum. Myometrial cell pairs were studied with respect to the total coupling conductance, the time and voltage dependence of macroscopic gap junction currents, sensitivity of the currents to the anesthetic agent halothane and to cyclic AMP, and properties of single gap junction channels. We report here that the mean gap junctional conductance in cell pairs from delivering animals was 4 to 10 times greater than in normal preterm or postpartum animals. The properties of gap junction coupling at different times in pregnancy were not found to differ significantly, except for the magnitude of the coupling conductance. Our observations support the idea that connexin-43 is a principal constituent of these channels in myometrium. However, the myometrial currents in some pairs exhibit an unusual degree of voltage dependence, suggesting either the presence of other connexins or novel properties of connexin-43.

MATERIALS AND METHODS

Isolation of myometrial paired cells

Paired cells were enzymatically isolated from the rat uterus at days 16, 19, and 22 (term), 1 day postpartum, and during preterm delivery after injection of RU-486 (mifepristone; Roussel-Uclaf, Paris, France). Preterm delivery was induced by the subcutaneous injection of 10 mg of the antiprogesterone RU-486 (in 150 μl benzyl benzoate and 350 μl castor oil) into day 18 pregnant rats; the animals were sacrificed 1 day later, when the onset of delivery was confirmed by the observation of at least one newborn pup. Mainly circular myometrium was used in this study, although previous intracellular work has focused upon the more easily obtained cells of the longitudinal muscle. The longitudinal and circular muscle layers differ in their electrical and biochemical properties (Bengtsson et al., 1984; El Alj et al., 1990), and, if anything, the electrical activity of the circular layer appears to undergo more drastic changes at parturition (Bengtsson et al., 1984). The uterus was dissected from timed pregnant rats (first-time pregnant, mated at 9 weeks of age; Sprague-Dawley, Charles River, Indianapolis, IN) under halothane anesthesia (after which the chest cavity of the still-anesthetized animal was opened to ensure proper euthanasia). After the endometrium was removed, strips of the circular muscle layer were carefully separated from the uterine muscle layers with fine scissors and cut into pieces less than 1 mm in length in ice-cold Hanks' solution (Gibco BRL, Gaithersburg, MD). The pieces of the muscle layer were washed by shaking for 15 min in 5 ml of low-Ca Hanks' solution at 37°C in a sterile Pyrex flask. The low-Ca Hanks' solution was made by adding 10 μM $CaCl_2$ to Ca- and Mg-free Hanks' solution (Gibco BRL). Each of four incubations with the enzyme solutions was performed with gentle shaking at 37°C for 20 min. During incubations 1 and 2, the enzyme solution consisted of 0.1 unit/ml collagenase (*V. alginolyticus*; Boehringer Mannheim Biochemica, Indianapolis, IN) and 2.3 units/ml dispase (Dispase I, *B. polymyxa*; Boehringer) in low-Ca Hanks' solution with 10 mM HEPES (Gibco BRL), pH 7.5. The purpose of using the solutions composed of purified enzymes is to minimize the exposure to the toxic proteolytic and lipolytic activities of the crude enzyme mixes (still required in steps 3 and 4 to obtain full dissociation). During incubations 3 and 4, the enzyme solution consisted of 0.1% collagenase (Type 4; Worthington Biochemical, Freehold, NJ), 0.01% hyaluronidase (Worthington), 0.01% elastase (Worthington), 0.01% soybean trypsin inhibitor (Worthington), and 0.1% fetal bovine serum albumin (Gibco BRL) in low-Ca Hanks' solution with 10 mM HEPES, pH 7.4. After removal of the enzyme solution, the cells and tissues were gently drawn back and forth through a large-pore pipette in low-Ca Hanks' solution. After the isolated cells settled to the bottom of the tube, the solution was removed. The cells were then stored in KB solution (Isenberg and Klöckner, 1982) at 4°C for a minimum of 1 h. The composition of KB solution was (mM): KCl 70.0, K_2HPO_4 20.0, $MgSO_4$ 5.0, pyruvate 5.0, taurine 20.0, creatine 5.0, succinate 5.0, K_2ATP 5.0, glucose 10.0, EGTA (Sigma Chemical, St. Louis, MO) 0.04, pH 7.2. Although many of the cells were completely dissociated to single cells, a small number of cells remained attached to one or more adjacent cells. Fig. 1 a shows a cell pair as it appeared in the experimental setup. Some cells, like those shown, were elongated in shape; however, many of the cells used were rounded; the results obtained did not differ based on cell shape. The cells were used within 6 h after isolation. The apparent input resistances of single cells isolated from circular muscle by these methods averaged 2.45 ± 0.95 GΩ (n = 10) using the Cs pipette solution (see Table 1; values given as mean ± SD). Because the seal resistances obtained are only a few gigaohms, the values of input resistance are underestimated, probably by a factor of 2 or so. The effective membrane capacitance of single cells was measured with the ramp pulse method to estimate the cell membrane area (Miyoshi et al., 1991). The values of membrane capacitance ranged from 40 pF to over 200 pF and did not change significantly between day 19 and day 22 in these preparations (p = 0.27, two-tailed t-test); thus no increase in cell size was apparent from these populations. Using a high-K internal solution, we determined the resting potential to be −39.8 ± 7.9 mV (n = 3). Similar values of resistance, capacitance, and membrane potential are obtained for longitudinal muscle (Miyoshi et al., 1991, unpublished data). Based on these values, the specific resistance R_m for these cells is approximately 2 to 5 × 10^5 Ω cm^2.

Immunofluorescent staining for connexin 43

For the staining of the freshly dissociated cells, a droplet of cells was placed into complete Medium 199 (Gibco BRL) inside a circle drawn with a PAP pen (Research Products International, Mount Prospect, IL) on a Superfrost/Plus slide (Fisherbrand, Fisher Scientific, Pittsburgh, PA) and incubated at 37°C in a CO_2 incubator. After 1 h, many of the cells adhered to the slide and the medium was gently replaced with phosphate-buffered saline (Amresco, Solon, OH). For the staining of intact muscle, frozen sections were prepared from the uteri of rats at days 18 and 22 of pregnancy. An anti-peptide antibody against rat connexin-43 was used for immunofluorescent staining of both tissue sections and cells, as previously described (Tabb et al., 1992; Sakai et al., 1992a).

Electrical recordings

The double-whole-cell voltage-clamp method was used to record gap junction currents between isolated myometrial paired cells visualized under

TABLE 1 Electrical properties of single freshly dissociated cells of circular myometrium

Parameters (pipette solution)*	Day 19	Day 22
Membrane capacitance (Cs)	96.3 ± 21.4 pF (n = 8)	81.7 ± 34.7 pF (n = 30)
Input resistance (Cs)	2.20 ± 0.57 GΩ (n = 4)	2.62 ± 1.16 GΩ (n = 6)
Input resistance (K)	—	1.53 ± 050 GΩ (n = 8)
Resting potential (K)	—	−39.8 ± 7.9 mV (n = 3)

*Cs, Cs internal solution; K, high-K internal solution.

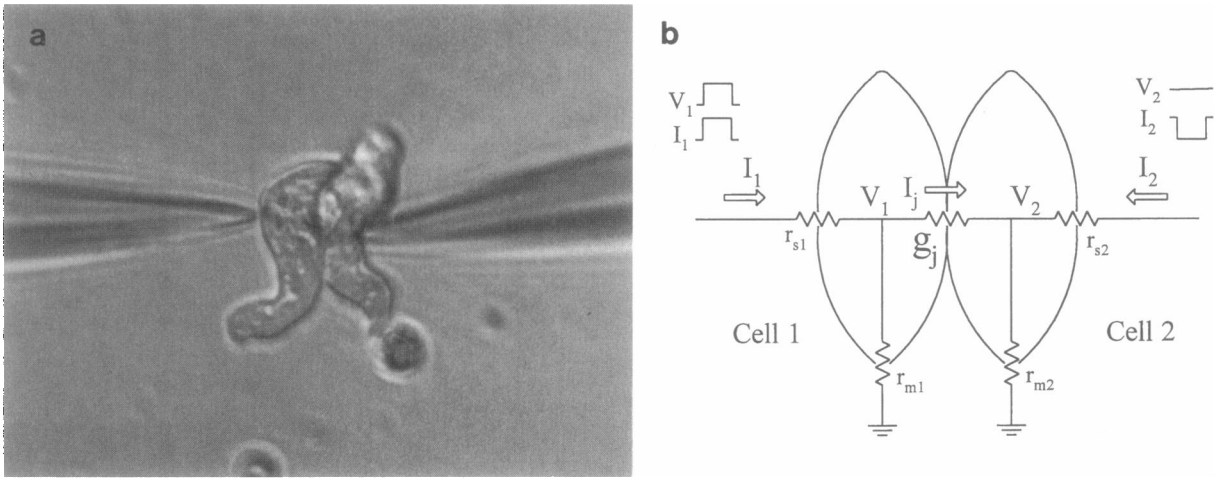

FIGURE 1 Paired cells and equivalent electrical circuit for the double patch-clamp method. (*a*) Paired cells viewed in the setup with a patch electrode on each cell. (*b*) Equivalent electrical circuit for the double patch-clamp method. I_1 (I_2) is injected current from the voltage amplifier no. 1 (no. 2). I_j is the junctional current and g_j is the junctional conductance. V_1 (V_2) is the membrane potential of cell 1 (cell 2) controlled by voltage clamp amplifier no. 1 (no. 2), and V_j is the transjunctional voltage. r_{s1} (r_{s2}) and r_{m1} (r_{m2}) are the series resistance and membrane resistance associated with cell 1 (cell 2). To a first approximation, the contributions of r_{m1} and r_{m2} can be ignored, if they are much larger than the junctional resistance ($= 1/g_j$).

a inverted microscope (Diaphot; Nikon, Tokyo, Japan). The conventional whole-cell patch-clamp method (Hamill et al., 1981) was applied to each cell of the pair (Neyton and Trautmann, 1985; White et al., 1985). Patch pipettes were fabricated from capillary tubes (glass type 7052; Garner Glass, Claremont, CA) using a pipette puller (PP-83; Narishige, Tokyo, Japan), and the tip was heat polished. The tip resistance of patch pipettes was measured to be in the range of 2.5 to 5 MΩ. In our experiments, each patch pipette is connected to a separate voltage clamp amplifier (Axopatch 200; Axon Instruments, Burlingame, CA). The test pulses are generated and currents are recorded on the computer connected to the DMA interface (TL-1, Axon), using the program of pCLAMP (Axon). The macroscopic currents were filtered through a 4-pole analog, low-pass bessel filter in the Axopatch 200 at a cutoff frequency of 5 KHz.

After achievement of the whole-cell patch-clamp configuration in both cells of a pair, the membrane potential in each cell is held at the same holding potential of 0 or −50 mV. The test pulses are injected into one cell (cell 1) while the membrane potential of the other cell (cell 2) is maintained at the holding potential (Fig. 1 *b*). To a first approximation, the transjunctional voltage (V_j) during a pulse was assumed to be the voltage difference between the test voltage and the holding potential ($V_1 - V_2$). The gap junction current (I_j) in response to V_j was recorded as the injected current ($-I_2$) to cell 2 from the voltage clamp amplifier. The (total) junctional conductance is defined as $g_j = I_j/V_j$.

Unitary gap junction currents were recorded from two groups of cells. One group is found spontaneously to have junctional conductances less than 0.5 nS. The other is composed of paired cells initially with much higher junctional conductances but having sufficiently attentuated cell coupling after halothane exposure, so that single-channel currents are resolved (Burt and Spray, 1989). The nominal concentration of halothane was 3.5 mM; however, the perfusion speed of the external solution was adjusted during single-channel recording to optimize the conductance. In most of the single-channel studies, the membrane potential of cell 1 was held at −50 mV, and cell 2 was at the holding potential of 0 mV, so that V_j was −50 mV. The single-channel events were recorded through the analog low-pass filter set at 1 kHz, with a sampling frequency of 250 Hz.

Voltage error due to series resistance

The voltage across the junction itself is less than the nominal command voltage, even at steady state, because of the voltage drop through the series resistance contributed by the two patch electrodes and the intracellular path. To estimate the magnitude of the series resistance error, a procedure similar to that for the recordings of gap junction currents was applied to a single myometrial cell instead of paired cells; here, two patch electrodes were placed on a single cell. The series resistance when recording from a single cell was assumed to be comparable to the series resistance due to two electrodes in the double patch-clamp method (Veenstra, 1990). The current amplitude in response to a 10-mV step pulse was measured and the apparent resistance, for the path through the two electrodes and the cytoplasm, was calculated. A lumped resistance value of 10.7 ± 1.4 MΩ (n = 9) was obtained from a single-cell recording. If the average series resistance is assumed to be 10 MΩ, the percentage error in the apparent junctional conductance should be substantial in some cases, and the larger conductances would tend to be preferentially underestimated. Our method does not take into account any access resistance immediately proximal to the junctional channels, such as that modeled by Wilders and Jongsma (1992), but the effect of ignoring this additional source of series resistance should be fairly small over the restricted range of g_j for which the voltage dependence was analyzed (<40 nS) in the present study. Such an access resistance causes junctional conductance to increase sublinearly as a function of channel number (see Discussion).

Data analysis

The relationship between the transjunctional voltage and the junctional conductance at the steady state was examined by fitting to the Boltzmann equation to determine the voltage dependence of the currents. The normalized conductance was fitted to the following equation:

$$G_j = ((G_{max} - G_{min}) / \{1 + \exp[-A(V_j - V_h)]\}) + G_{min},$$

where G_j is the normalized value of junctional conductance. G_{max} is the maximum value of G_j and is set to be 1. G_{min} is the value of G_j at the steady state. V_h is the half inactivation voltage (mV) at which G_j is reduced by 50% of ($G_{max} - G_{min}$), and A is the slope factor (mV^{-1}). Curve fitting was carried out using the Marquardt-Levenberg algorithm in SigmaPlot (Jandel Scientific, San Rafael, CA).

Unitary junctional conductance was determined in two ways, which yielded closely similar results: 1) from amplitude histograms of all data points or 2) from the amplitudes of identified single-channel events compiled into a histogram. The data were preprocessed with a digital Gaussian filter at 50 Hz in pCLAMP. The histogram data were fitted to a sum of

Gaussian distribution functions using a curve-fitting program in SigmaPlot. Then the unitary junctional conductance was determined as the peak values of these functions.

Results for the measurements are expressed as mean ± SD (n = number of observations). The Kruskal-Wallis ANOVA test was used to examine the statistical significance of the differences between days of pregnancy. Dunn's Multiple Comparisons Test was used as a post-test to determine which medians were significantly different from one another. A nonparametric approach was preferred to analyze the data in Fig. 3, because some groups (days 16 and 19) failed the assumption of normality.

Solutions

For electrical recording, a low-Ca external (bath) solution and a Cs internal (pipette) solution were used. The concentration of Ca is low in both solutions, and internal Cs ions are substituted for K ions to reduce the effects of Ca and K channel currents. The composition of the low-Ca external solution was (mM): NaCl 140.0, KCl 5.4, $CaCl_2$ 0.1, $MgCl_2$ 5.0, glucose 11.0, HEPES 5.0, pH 7.4. The Cs internal solution contained (mM): CsCl 110.0, NaCl 5.0, $MgCl_2$ 5.0, K_2ATP 5.0, creatinine phosphate sodium salt 5.0, KH_2PO_4 1.0, EGTA 5.0, glucose 5.5, HEPES 5.0, pH 7.2. Reagents, including isoproterenol and dibutyryl cyclic AMP, were obtained from Sigma. All experiments were conducted at room temperature.

RESULTS

Immunofluorescent staining for connexin-43

The presence of gap junctions containing connexin-43 is readily demonstrated by extensive punctate immunostaining at contact sites between adjacent cells in myometrial tissues at term delivery on day 22 (Fig. 2 *a*), but not in preterm, nonlaboring animals before day 22 (Fig. 2 *b*, day 18; Tabb et al., 1992). Fig. 2, *c* (day 22 delivery) and *d* (day 19), show a similar comparison for freshly dispersed myometrial cells. Unlike cultured cells, most of the freshly dissociated cells have not flattened out and thus tend toward higher background. Connexin-43 staining in the form of small bright spots was seen in the freshly dissociated pairs from day 22 animals, but only to a much lesser extent in cells from day 19. The spots seemed to concentrate over the regions of apparent contact of cells. Some spots could also be seen in distal regions, not unexpectedly, because the cells isolated in pairs were probably coupled to additional cells before the dissociation. Staining located at a distance from contact of

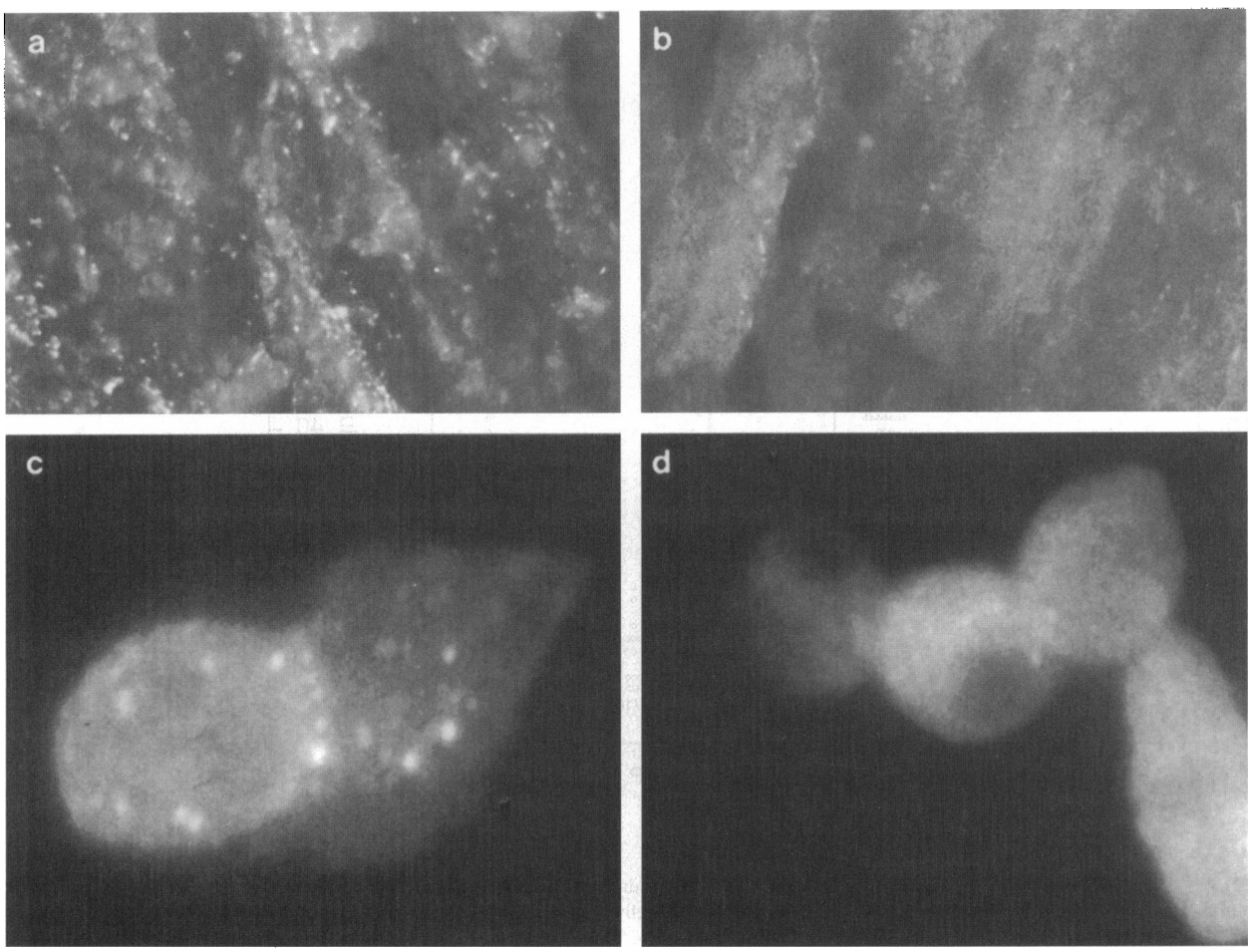

FIGURE 2 Immunofluorescent staining for connexin 43. Myometrial tissue stained by connexin-43 antibody and an FITC-labeled secondary antibody is demonstrated at day 22 delivery in *a* and at day 18 in *b*. For *c* and *d*, paired cells were freshly isolated from the uterine circular layer of pregnant rat. Bright spots of fluorescent staining with connexin-43 antibody are evident. The spots are greater at day 22 delivery (*c*) in both number and size compared with day 19 (*d*).

the two cells may represent remnants of gap junctions destroyed during the dissociation. The isolated cells, like the intact tissue, stain more heavily for connexin-43 at term than earlier in pregnancy, supporting their use as a model system for studying changes in junctional coupling.

Magnitude of junctional conductance in myometrial paired cells at different times in pregnancy

To estimate macroscopic junctional conductance, 300-ms step pulses of ±10 mV (V_1) were applied to record junctional currents (I_j estimated as $-I_2$; Fig. 1 *b*) between the cells; both cells were held at 0 mV. At $V_j = \pm 10$ mV, junctional currents were essentially noninactivating.

The junctional conductances as measured in cell pairs from day 16, day 19, RU-486-treated preterm delivering, day 22 predelivery, day 22 delivery, and 1 day postpartum are plotted in Fig. 3. The left-hand panel represents pairs from the circular layer; the right, pairs from the longitudinal layer. Each nonzero measurement is represented as an open symbol; for clarity, however, the "zero" ($g_j < 20$ pS) values are represented by a single open rectangle rather than individually. The quantity (*n*/*m*) beneath each dataset represents the number of cell pairs with "zero" coupling (*n*) and total cell pairs studied (*m*). Error bars (average value ± SD) are shown to the right of each group of points.

Even without corrections for series resistance, the average value of junctional conductance between circular muscle cells on day 22 (32 ± 16 nS) was about 7 times higher than on day 19 (4.6 ± 7.9 nS), supporting our hypothesis that the myometrial cells undergo a substantial increase in electrical coupling before the onset of labor. Assuming a series resistance of 10 MΩ for the present experiments, these average values of 4.6 and 32 nS would be corrected to 4.8 and 47 nS, with errors of ~5% and 42%, respectively, indicating that the noncorrected values may underestimate the conductance change over the last few days of pregnancy. The values for days 22 predelivery, 22 delivering, and RU-486-injected preterm delivering were significantly higher than for days 16 and 19 and postpartum. The coupling in cell pairs from animals at 1 day postdelivery was only 6.5 ± 10 nS, implying that the increased coupling disappears quickly after delivery.

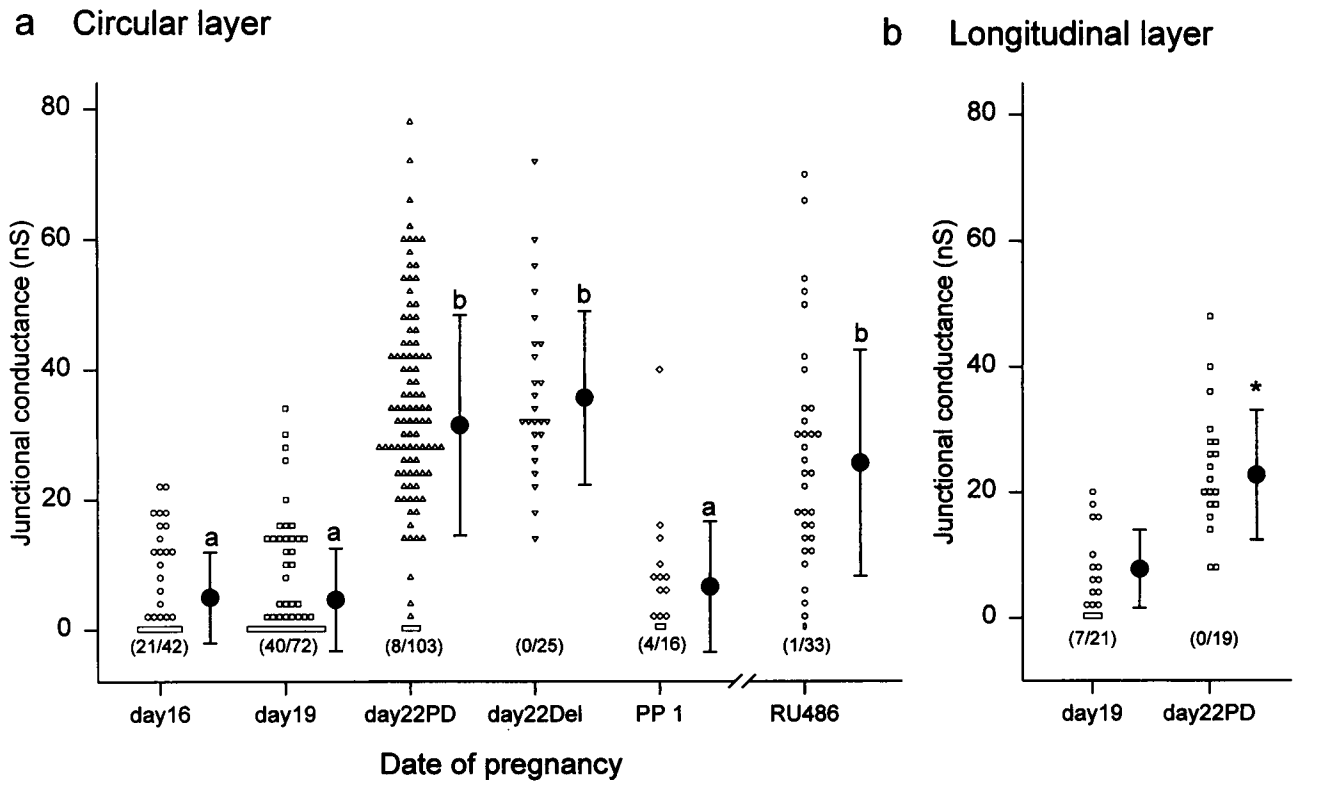

FIGURE 3 Change of junctional conductance during pregnancy. (*a*) Individual measurements of junctional conductance from circular-muscle pairs are plotted for day 16, day 19, day 22 predelivery (day22PD), day 22 actively delivering (day22Del), 1 day postpartum (PP1), and day-19 preterm-delivering (RU486). Nonzero values are plotted individually as open symbols; for clarity, "zero" values are represented as single open boxes for each group. ●, Mean values of junctional conductance, with error bars (mean ± SD). Differences among the six groups were significant at the $p < 0.0001$ level. By Dunn's test, there were two sets of means, days 16 and 19, and postpartum (marked a), and days 22 predelivery and delivering and preterm delivering (RU486) (marked b). Means within the same set are not significantly different; all other pairwise comparisons of means are different at the $p < 0.05$ level of significance. (*b*) In cells from the longitudinal layer, also, average junctional conductance was higher for the day 22 cells than day 19 ($p < 0.05$, two-tailed *t*-test). The number of rats per group ranged from 3 to 31.

Fig. 3 *b* compares preterm and term pairs from the longitudinal muscle layer, demonstrating a similar, roughly fourfold, increase in junctional conductance between days 19 and 22.

Voltage dependence of gap junction currents

For analysis of voltage dependence, gap junction currents were recorded from paired cells from circular muscle using 5-s step pulses between ±90 mV in 20-mV increments, as shown in Fig. 4. To limit the errors introduced by series resistance, only pairs with junctional conductance less than 40 nS were included for the analysis of voltage dependence. Similar results were obtained with holding potentials of either 0 or −50 mV, indicating, as expected, that the transjunctional voltage is more important than the transmembrane potential per se in gating junctional channels.

Fig. 4 shows the gap junction currents recorded from two day 22 cell pairs. In all cases, gap junction currents decayed to a steady-state level gradually at most test voltages, but were not inactivated completely even by the largest test voltages. Plots of current at very early times after the onset of the test step were linear, showing that the instantaneous conductance was constant. The conductance decreased in a time- and voltage-dependent manner for large transjunctional voltages, causing the current to decay over hundreds of milliseconds or longer. These results are generally similar to published data for other gap junctions in other tissues predominantly expressing connexin-43 (Wang et al., 1992; Moreno et al., 1993; Moreno et al., 1994). The time course of the decline in the currents was fitted more satisfactorily by a sum of two exponentials rather than by a single exponential function.

However, the cell pairs could be divided into two populations, based on two types of voltage dependence that were observed with equal frequency. Type I currents, exemplified by Fig. 4, *a* and *b*, closely resembled currents seen in other preparations, such as heart, where connexin-43 predominates. The voltage-dependent decrease in the steady-state currents in Type I pairs is small until the transjunctional driving force is 50 mV or greater. The Type II pairs (Fig. 4, *c* and *d*), by contrast, showed a marked voltage dependence at small transjunctional voltages. This degree of voltage dependence is not expected for gap junctions composed of connexin-43, but it is reminiscent of the currents associated with connexin-45 (Discussion).

The essential characteristics of gap junction currents (other than magnitude) appear not to change in the late stages of pregnancy. In particular, Type I and Type II cell pairs were found with approximately equal frequency on days 19 and 22.

For Fig. 5, average steady-state conductances were derived from four Type I and four Type II cell pairs (selection

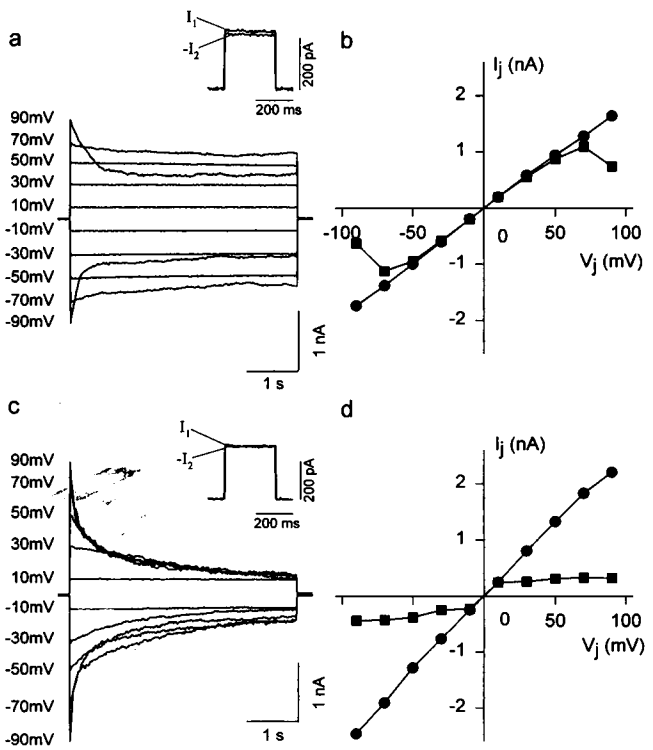

FIGURE 4 Families of gap junction currents and the current-voltage relationship in day 22 cell pairs. Two types of currents (I, II) are shown in *a-b* and *c-d*, respectively. (*a*, *c*) Gap junction currents in response to 5-s step pulses in the voltage range of ±90 mV. (*b*, *d*) The instantaneous (●) and steady-state (■) currents are plotted against transjunctional voltages. By contrast with *b*, the steady-state conductance in *d* declines for $|V_j| \leq 30$ mV.

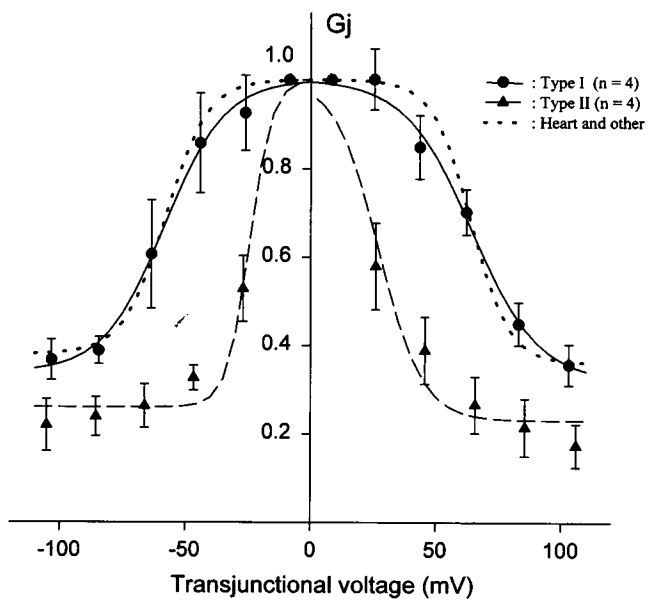

FIGURE 5 Conductance-voltage relationship. The mean values of normalized junctional conductance at the steady state are plotted as a function of transjunctional voltage (●) with error bars (mean ± SE). The values of junctional conductance were calculated from current amplitudes at the steady state in four Type I and four Type II pairs (day 22 predelivery). Each solid curve was drawn by fitting the averaged data to the Boltzmann function; the resulting fit parameters are listed in Table 2. The dotted line was drawn using the parameters (also in Table 2) of Moreno et al. (1994).

criterion: $g_j < 40$ nS) from day 22 uterus. The junctional conductances in the Type I (mean $g_j = 18.3 \pm 9.8$ nS) and Type II (24.4 ± 12.9) cell pairs were similar. Input resistances estimated roughly from the cell 1 currents (Fig. 4, inset) for each pair were also similar: 1.7 ± 2.2 GΩ (Type I) versus 2.0 ± 2.1 GΩ (Type II). For this plot, the command voltages were corrected for series resistance by assuming a value of 10 MΩ; this correction changed the shape of the curves slightly. Each conductance-voltage relationship was bell shaped, as expected, and was fitted by a Boltzmann relation (solid line). The parameters (±SE) needed to fit the data are shown in Table 2. V_h and G_{min} for the Type II myometrial pairs were smaller than for Type I. The Type II cell data may not be as well fit by this Boltzmann equation as the Type I data.

The dotted line represents the results of an analysis carried out by Moreno et al. (1994) for gap junctions in heart and in corpus cavernosum smooth muscle, both of which mainly express connexin-43, and for connexin-43 channels expressed in cultured SKHep1 cells. Like many other investigators (Veenstra et al., 1992; Wang et al., 1992), they found that the gap junction currents show little voltage dependence until the transjunctional potential exceeds ±50 mV, as indicated by the flatness of the fitted curve at smaller voltages. Our Type I cell data fall close to their curve. By contrast, the Type II data show gating at lower transjunctional voltages, indicated by the much sharper peak of the solid curve. The overall effect of the increased voltage dependence is that channel gating will occur, on average, at more modest transjunctional voltages in the myometrium.

Effects of halothane on gap junction currents

The effects of halothane, an anesthetic agent known to decrease cell-cell coupling, on junctional conductance were investigated. Halothane finds some use in obstetrics because of its ability at very high concentrations (equivalent to a few millimolar in physiological fluids, Jing et al., 1995) to produce the profound relaxation of the uterus needed for intrauterine manipulation (Cunningham et al., 1993). As shown in Fig. 6, when halothane at a nominal concentration of 3.5 mM was applied externally to paired cells, gap junction currents were rapidly reduced to low levels. Once cell pairs were treated in this way, no junctional currents could be recorded between paired cells and the apparent coupling resistance increased to >50 GΩ. After wash-out of halothane, the current recovered rapidly. At the beginning of the recovery phase, or with sustained application of lower concentrations of halothane, small numbers of individual channels were routinely observed (Burt and Spray, 1989) and could be studied.

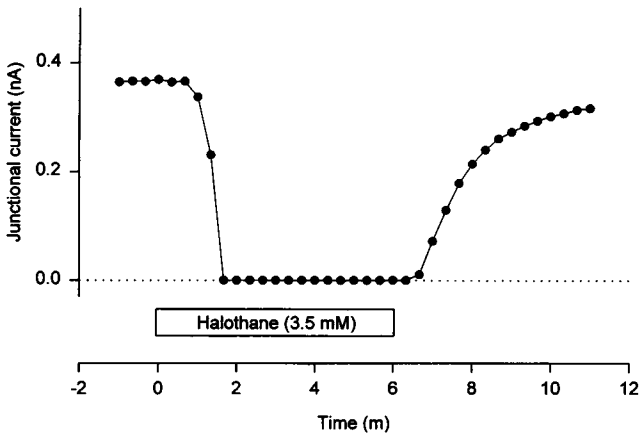

FIGURE 6 The effect of halothane on junctional conductance. The changes in junctional conductance during halothane exposure were examined by measuring the amplitudes of gap junction currents from a day 22 (predelivery) pair in response to 300-ms step pulses of −10 mV every 20 s from a holding potential of 0 mV. Before the exposure the current amplitudes were constant for 5 min.

Effects of cAMP and isoproterenol on junctional currents

Previous studies have suggested that β-adrenergic agents have the ability to reduce coupling in myometrium (Sakai et al., 1992b; Cole and Garfield, 1986). To test this idea further, coupled cell pairs were treated with isoproterenol and dibutyryl-cAMP, as illustrated in Fig. 7, using the same pulse protocol as in Fig. 6. Before the drug was applied, the current was stable for at least 5 min; in temporal control experiments where no drug was applied, no changes in current occurred over at least an additional 10 min. For each agent, a decrease of about 15% in the junctional current was observed. The small size of the second-messenger-mediated responses is not surprising, as it echoes the experience of many other investigators using whole-cell methods (e.g., Moore et al., 1991; Moreno et al., 1993). These small responses probably reflect the depletion through the pipette opening of intracellular components needed for the response (Horn and Marty, 1988).

TABLE 2 Parameters for the fit of voltage dependence of junctional conductance to the Boltzmann equation

	Negative V_j			Positive V_j		
	G_{min}	V_h (mV)	A (mV^{-1})	G_{min}	V_h	A
Type I	0.34 ± 0.02	−58.5 ± 1.8	0.08 ± 0.01	0.32 ± 0.04	64.4 ± 2.9	−0.07 ± 0.01
Type II	0.26 ± 0.02	−24.6 ± 1.5	0.23 ± 0.11	0.23 ± 0.04	27.3 ± 3.2	−0.11 ± 0.04
Moreno et al. (1994)	0.38	−58	0.12	0.36	64	−0.13

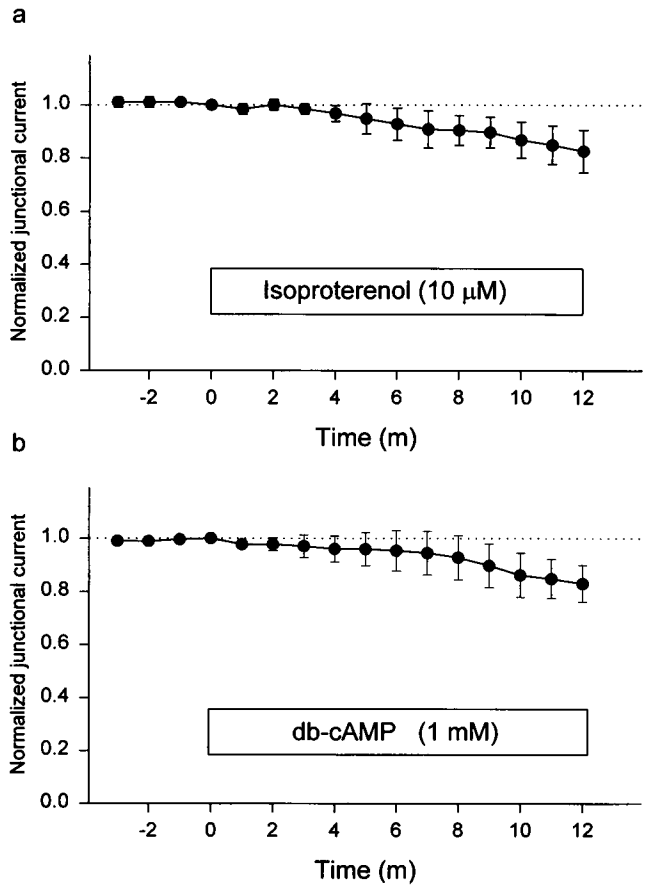

FIGURE 7 The effect of isoproterenol and db-cAMP on junctional conductance. The effect of isoproterenol and db-cAMP on the amplitudes of gap junction currents was tested using a day 22 (predelivery) pair. Before these drugs were applied, the current amplitudes were constant for 5 min. Junctional currents were normalized to the current amplitude at the beginning of drug exposure, and the mean values (± SD) were plotted at 1-min intervals. (*a*) Isoproterenol (10 μM) was applied in the bath solution and the current was reduced by 17.0 ± 6.9% (n = 4). (*b*) Similarly, db-cAMP (1 mM) blocked the currents by 17.3 ± 8.0% (n = 5).

Unitary conductances of gap junction currents

A few myometrial pairs had a junctional conductance of <0.5 nS, so it was possible to resolve single channels without halothane pretreatment. In these cases, the currents consisted of step fluctuations from the baseline, interpreted as unitary gap junction channel currents. A family of small gap junction currents elicited during test steps to various transjunctional voltages (from a holding potential of 0 mV) is shown in Fig. 8 *a*. In Fig. 8 *b*, the amplitude histogram for all data points obtained for V_j = 50 mV is shown. The data was fit by a sum (dots) of four Gaussian curves (solid lines), centered at 0, 90, 192, and 212 pS. The fit suggests that one unitary conductance is around 90 pS and another conductance is about 20 pS. In Fig. 8 *c*, the data were reanalyzed by identifying each channel opening event at each test voltage. The slope of the fitted line, which represents the unitary current levels due to a single open channel of the most frequently observed size, was calculated to be 88 pS. Larger amplitudes probably resulted from the simultaneous opening of two 88-pS channels; the smaller amplitudes of unitary currents, detected at some test voltages, suggest the presence of another, lower conductance state.

Further analysis of unitary junctional conductance was made from myometrial paired cells exposed to halothane to reduce coupling, allowing the observation of single channels. Recordings of unitary gap junction currents at V_j of −50 mV are shown in Fig. 9 *a*. Two single-channel current amplitudes can be observed in these traces (shown inverted). The large conductance was calculated to be about 85 pS and the smaller one was about 25 pS. To determine more systematically the value of unitary junctional conductance, the amplitudes of single-channel events identified at −50 mV in 13 pairs of cells were measured and plotted in amplitude histograms. For day 22 (Fig. 9 *b*), peak values of unitary junctional conductance were 84.8 and 24.2 pS, and 85.3% of the events were included in the larger conductance category. At day 19 (Fig. 9 *c*), peak values were 83.3 and 28.8 pS, and 90.0% of the events were in the larger category. The mean values of the junctional conductance under halothane exposure are similar to those measured from the untreated pairs with small conductance.

DISCUSSION

This study demonstrates that the increased incidence of gap junctions between cells of the uterine myometrium during term and preterm labor is mirrored by an increase in functional coupling. When the expected errors due to series resistance are taken into account, our data suggest that the coupling conductance between adjacent cells may increase by roughly an order of magnitude near the time of delivery (either preterm or term), returning to lower levels in the first day postpartum. Structural studies have suggested an even greater relative increase in coupling. However, functional studies may generate a truer picture of coupling than structural studies, because the effective access resistance near the channels may cause the conductance to increase sublinearly with numbers of channels (Wilders and Jongsma, 1992).

The major assumption of the present study is that the junctions we study in dissociated cells represent the population of junctions in intact muscle, an assumption supported by immunostaining (Fig. 2). The rationale for using freshly dissociated cells rather than cultured cells is that important changes occur very rapidly around the time of labor, indicating a potential for lability. The gap junction proteins themselves turn over rapidly (Saffitz et al., 1995). Because the dissociated cells are kept at 4°C until use, it seems unlikely that many new junctions could form, so the junctions studied here should be a subset of the original junctions. Whether, during dissociation, junctions are lost disproportionately from cells from different stages of gestation is unclear. Because gap junctions may have some mechanical function in stabilizing cell contacts, cells with fewer or smaller gap junctions may more easily lose them.

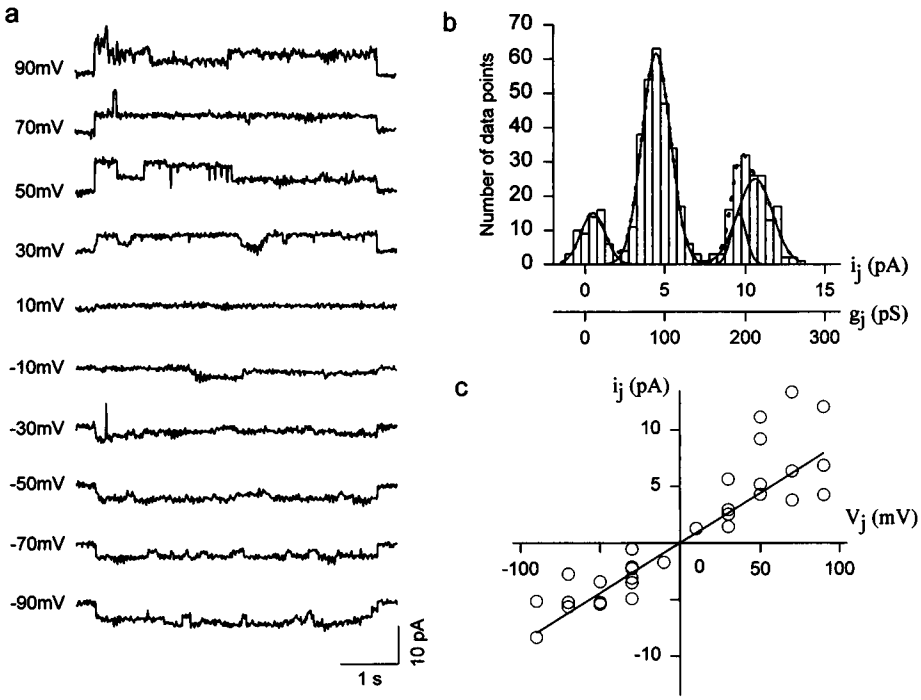

FIGURE 8 Single-channel currents in weakly coupled paired cells. (*a*) Step pulses of 5 s in the range of ±90 mV were applied to day 22 paired cells with $g_j < 0.5$ nS. In this case small step currents were recorded at each voltage, suggesting that a few gap junction channels were active between the pair and had two states, open and closed. The transjunctional voltage is shown to the left of each current. (*b*) Amplitude histogram of all data points in the current at V_j of 50 mV separated in 0.5-pA (10 pS) bins. The abscissa is current amplitude. The number of digitized data points is 512. The solid lines represent individual Gaussian curves; the dotted lines represent the sum of the fitted curves. The fitted peaks are at ~0, 4.5 pA (90 pS), 9.6 pA (192 pS), and 10.6 pA (212 pS). (*c*) The amplitudes of identified openings are plotted against transjunctional voltages. The line is fitted to the data representing a single open channel of 88 pS.

Although there is no evidence that this occurred, this effect could, in principle, have caused us to underestimate the day 16, day 19, and postpartum gap-junction conductances preferentially, thereby inflating the difference between the delivering and nondelivering groups. However, this effect could not invalidate our basic conclusions.

The functional significance of the increased gap junctional coupling has previously been discussed in terms of enhanced propagation and synchronization of electrical activity (Garfield et al., 1978; Miller et al., 1989). Among spontaneously active smooth muscles, the plasticity of cell-to-cell coupling is apparently unique to the uterus. The regulation of gap junction coupling is thought to determine uterine electrical activity in two ways. First, preterm, uterine quiescence is enforced by limiting the flow of excitation from cell to cell. Second, during labor, an increased amount of coupling is needed for robust contractile activity. It is essentially axiomatic that more gap junctions will enhance cell-to-cell communication; however, the new gap junctions could fail to be important if they do not open or their incremental contribution to improved coupling is not significant. The present study argues against the idea that the junctions are nonfunctional. The question is, how large a difference do they make? No one knows. Many changes occur during parturition, and understanding the relative contribution due to new gap junctions as opposed to new channels of other types and additional factors affecting electrical parameters will require further study.

However, assuming for the sake of argument that the increase in gap junctions is the predominant factor, what can be concluded from a comparison of propagation at term versus preterm? Increased propagation might be demonstrated as an increase in either the velocity of propagation or the distance over which propagation occurs. Miller et al. (1989) studied the propagation of spontaneous activity in muscle strips in vitro and found both propagation velocities and distances at term to be about 2 or 3 times the preterm values. Their findings show a net increase in propagation at term, the expected effect of increased junctional conductance.

Is it plausible that the increased gap junctions have a strong facilitatory effect, or is it more likely that the preexisting junctions, at their preterm levels, have a maximum effect? The ratio of plasma membrane resistance in a single cell to gap junction resistance should indicate the effectiveness of propagation of activity from one cell to the next. If we assume an input resistance at rest of 5 GΩ for these cells, this ratio increased from roughly 10 in nondelivering pairs (but with a disproportionate number of "zeros") to 100 near delivery. Similar values for this ratio (10–100) are found for paired heart cells (Wilders and Jongsma, 1992). Without "corrections" for the average number of cells to which each cell is coupled, this analysis is not completely valid; for example, when the average number of coupled neighbors increases, the effective electrical load seen by a cell will increase, even for constant cell sizes. Clearly, however, the input resistance of myometrial cells is much higher than gap junction resistances, suggesting that current flow between coupled cells is favored, even preterm. It is thought that only a few channels are sufficient for action potential transfer from one cell to another; however, the effect of an increasing ratio of junctional to nonjunctional conductance on full frequency and waveform entrainment is probably more complicated (Weingart and Maurer, 1988; Cai et al., 1994). Furthermore, the many "zeros" observed preterm suggest that even the requirement for a "few channels" may

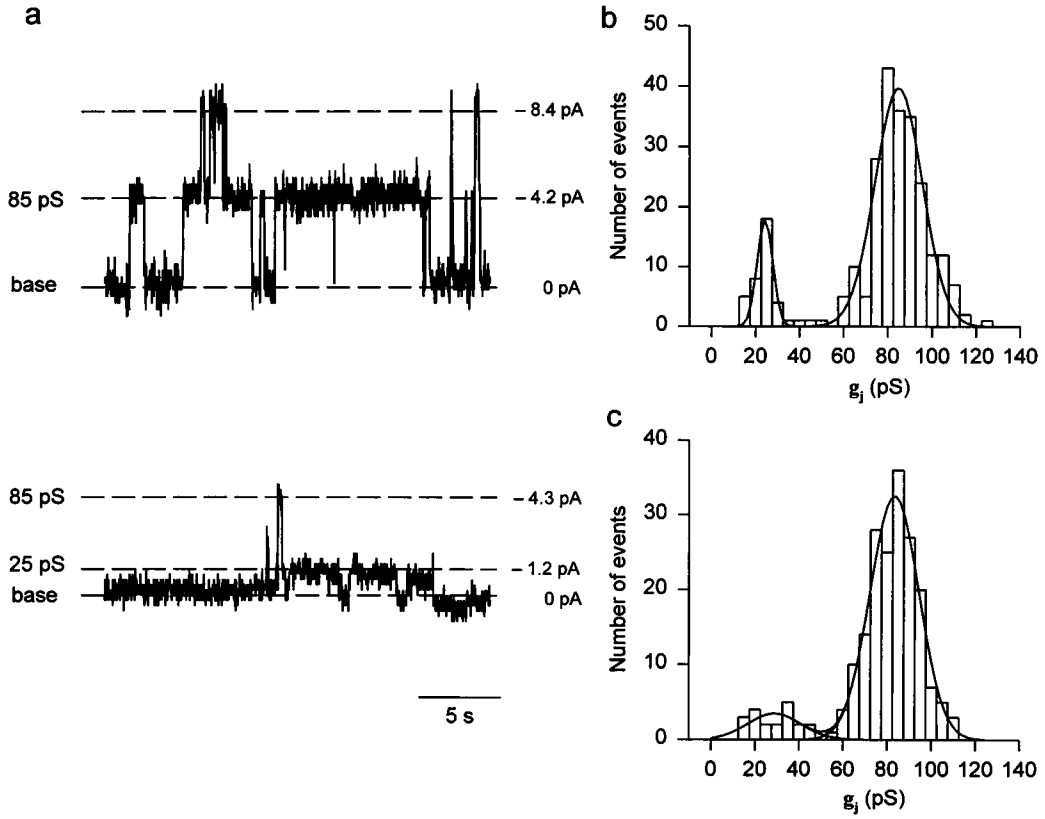

FIGURE 9 Single-channel currents from day 22 (predelivery) and day 19 paired cells under halothane exposure. (*a*) Single-channel currents at a V_j of −50 mV are shown (negative current upward, day 22). Step currents due to one or two simultaneous openings of gap junction channels were observed (top trace). Two sizes of junctional conductance were detected: 85 and 25 pS (bottom trace). (*b*) Amplitude histogram of day 22 single-channel events (259 events in 10 pairs) arranged in 5-pS bins. The peaks are 84.8 and 24.2 pS. (*c*) The data for day 19 were derived from 200 events in three pairs. The peaks are 83.3 and 28.8 pS. When the data in *b* and *c* are combined, the peaks are at 84.2 and 23.7 pS (not shown).

not be fulfilled before term. We hypothesize, then, that the additional gap junctions are important in increasing the electrical coupling, to increase the coordination, rate, and thoroughness of invasion of activity through the muscle, possibly against substantial increases in the electrical load.

In many, but not all, respects, the properties of the myometrial gap junctions conform to what has been described for other tissues predominantly expressing connexin-43. From the observed single-channel conductances of 85 and 25 pS, our data suggest that connexin-43 is the predominant connexin. A variety of observed channel sizes have been explained as variant states of connexin-43 channels, including 60 pS (e.g., heart; Burt and Spray, 1988) and 90 and 30 pS (e.g., smooth muscle; Moore et al., 1991; Moreno et al., 1993). The 30-pS channels have been posited to represent a voltage-insensitive substate of the connexin-43 channel, accounting for the residual, voltage-insensitive channel activity underlying G_{min} (Moreno et al., 1994).

Alternatively, the 30-pS channels we observed may reflect the presence of connexin-45, which is more voltage sensitive (Saffitz et al., 1995). The degree of voltage dependence of the Type II current is difficult to reconcile with other data on other adult tissues predominantly expressing connexin-43 (Wang et al., 1992; Moreno et al., 1994). Our Type II macroscopic current findings most resemble of those of Veenstra and co-workers (1992), who studied the properties of coupling in heart myocyte pairs from chick embryos. The voltage dependence in chick was explained by the expression of connexin-42 and connexin-45, rather than connexin-43. In our studies, the 30-pS channels represent a minor component of the activity (10–15%) in any given cell pair, however, and seem unlikely to dominate the macroscopic current. Our Type II findings may alternatively represent a novel degree of voltage dependence for currents through gap junction channels composed mostly of connexin-43. In laboring uterine muscle, where the slow depolarizing waves and action potential bursts last tens of seconds, the very slow gating of cell-cell coupling could significantly affect the electrical activity and even help to terminate the contraction, if sufficiently long-lasting differences in intracellular voltage in adjacent cells occur.

Because the selective inhibition of gap junction currents in uterus should be a definitive treatment for preterm labor, the actions of agents that can reduce junctional coupling are being explored. The clinical usefulness of halothane is limited to fairly rare situations where full uterine relaxation is needed (Cunningham et al., 1993). The effects of β-adrenergic agents, used to inhibit preterm contractions, are not

maintained during continuous administration, but may be effective for weeks if given episodically. The inhibition by cAMP of gap junction currents in uterus is in marked contrast to the elevation of junctional conductance in cardiac cells (Spray and Burt, 1990).

Taken together, these findings extend our understanding of the importance of increased cell-cell coupling in the myometrium to the onset and success of labor. Quantitative data for junctional and membrane conductances may play an important role in reconstructing the uterine electromyogram, a tool that is showing promise for the diagnosis of term and preterm labor in women (Buhimschi and Garfield, 1996).

Supported by a grant from the March of Dimes Birth Defects Foundation to REG.

REFERENCES

Bengtsson, B., E. M. Chow, and J. M. Marshall. 1984. Activity of circular muscle of rat uterus at different times in pregnancy. *Am. J. Physiol.* 246:C216–C223.

Buhimschi, C., and R. E. Garfield. 1996. Uterine contractility as assessed by abdominal surface recording of electromyographic activity in rats during pregnancy. *Am. J. Obstet. Gynecol.* 174:744–753.

Burt, J. M., and D. C. Spray. 1988. Single-channel events and gating behavior of the cardiac gap junction channel. *Proc. Natl. Acad. Sci. USA.* 85:3431–3434.

Burt, J. M., and D. C. Spray. 1989. Volatile anesthetics block intercellular communication between neonatal rat myocardial cells. *Circ. Res.* 65: 829–837.

Cai, D., R. L. Winslow, and D. Noble. 1994. Effects of gap junction conductance on dynamics of sinoatrial node cells: two-cell and large-scale network models. *IEEE Trans. Biomed. Eng.* 41:217–231.

Cole, W. C., and R. E. Garfield. 1986. Evidence for physiological regulation of myometrial gap junction permeability. *Am. J. Physiol.* 251: C411–C420.

Cole, W. C., R. E. Garfield, and J. S. Kirkaldy. 1985. Gap junctions and direct intercellular communication between rat uterine smooth muscle cells. *Am. J. Physiol.* 249:C20–C31.

Cunningham, F. G., P. C. MacDonald, N. F. Gant, K. J. Leveno, and L. D. Gilstrap, III, eds. 1993. Williams Obstetrics, 19th Ed. Appleton and Lange, Norwalk, CT.

El Alj, A., E. Bonoris, E. Cynober, and G. Germain. 1990. Heterogeneity of oxytocin receptors in the pregnant rat myometrium near parturition. *Eur. J. Pharmacol.* 186:231–238.

Garfield, R. E., C. P. Puri, and A. I. Csapo. 1982. Endocrine, structural, and functional changes in the uterus during premature labor. *Am. J. Obstet. Gynecol.* 142:21–27.

Garfield, R. E., S. Sims, and E. E. Daniel. 1977. Gap junctions: their presence and necessity in myometrium during parturition. *Science.* 198: 958–960.

Garfield, R. E., S. M. Sims, M. S. Kannan, and E. E. Daniel. 1978. Possible role of gap junctions in activation of myometrium during parturition. *Am. J. Physiol.* 235:C168–C179.

Hamill, O. P., A. Marty, E. Neher, B. Sakmann, and F. J. Sigworth. 1981. Improved patch-clamp techniques for high-resolution current recording from cells and cell-free membrane patches. *Pflugers Arch.* 391:85–100.

Hendrix, E. M., S. J. Mao, W. Everson, and W. J. Larsen. 1992. Myometrial connexin 43 trafficking and gap junction assembly at term and in preterm labor. *Mol. Reprod. Dev.* 33:27–38.

Horn, R., and A. Marty. 1988. Muscarinic activation of ionic currents measured by a new whole-cell recording method. *J. Gen. Physiol.* 92:145–159.

Isenberg, G., and U. Klöckner. 1982. Calcium tolerant ventricular myocytes prepared by preincubation in a "KB medium." *Pflugers Arch.* 395:6–18.

Jing, M., J. L. Hart, E. Masaki, R. A. Van Dyke, S. Bina, and S. M. Muldoon. 1995. Vascular effects of halothane and isoflurane: cGMP dependent and independent actions. *Life Sci.* 56:19–29.

Lang, L. M., E. C. Beyer, A. L. Schwartz, and J. D. Gitlin. 1991. Molecular cloning of a rat uterine gap junction protein and analysis of gene expression during gestation. *Am. J. Physiol.* 260:E787–E793.

Miller, S. M., R. E. Garfield, and E. E. Daniel. 1989. Improved propagation in myometrium associated with gap junctions during parturition. *Am. J. Physiol.* 256:C130–C141.

Miyoshi, H., T. Urabe, and A. Fujiwara. 1991. Electrophysiological properties of membrane currents in single myometrial cells isolated from pregnant rats. *Pflugers Arch.* 419:386–393.

Moore, L. K., E. C. Beyer, and J. M. Burt. 1991. Characterization of gap junction channels in A7r5 vascular smooth muscle cells. *Am. J. Physiol.* 260:C975–C981.

Moreno, A. P., A. C. Campos de Carvalho, G. Christ, A. Melman, and D. C. Spray. 1993. Gap junctions between human corpus cavernosum smooth muscle cells: gating properties and unitary conductance. *Am. J. Physiol.* 264:C80–C92.

Moreno, A. P., M. B. Rook, G. I. Fishman, and D. C. Spray. 1994. Gap junction channels: distinct voltage-sensitive and -insensitive conductance states. *Biophys. J.* 67:113–119.

Neyton, J., and A. Trautmann. 1985. Single-channel currents of an intercellular junction. *Nature.* 317:331–335.

Noma, A., and N. Tsuboi. 1987. Dependence of junctional conductance on proton, calcium and magnesium ions in cardiac paired cells of guinea-pig. *J. Physiol. (Lond).* 382:193–211.

Petrocelli, T., and S. J. Lye. 1993. Regulation of transcripts encoding the myometrial gap junction protein, connexin-43, by estrogen and progesterone. *Endocrinology.* 133:284–290.

Risek, B., S. Guthrie, N. Kumar, and N. B. Gilula. 1990. Modulation of gap junction transcript and protein expression during pregnancy in the rat. *J. Cell Biol.* 110:269–282.

Saffitz, J. E., L. M. Davis, B. J. Darrow, H. L. Kanter, J. G. Laing, and E. C. Beyer. 1995. The molecular basis of anisotropy: role of gap junctions. *J. Cardiovasc. Electrophysiol.* 6:498–510.

Sakai, N., T. Tabb, and R. E. Garfield. 1992a. Studies of connexin 43 and cell-to-cell coupling in cultured human uterine smooth muscle. *Am. J. Obstet. Gynecol.* 167:1267–1277.

Sakai, N., T. Tabb, and R. E. Garfield. 1992b. Modulation of cell-to-cell coupling between myometrial cells of the human uterus during pregnancy. *Am. J. Obstet. Gynecol.* 167:472–480.

Sims, S. M., E. E. Daniel, and R. E. Garfield. 1982. Improved electrical coupling in uterine smooth muscle is associated with increased numbers of gap junctions at parturition. *J. Gen. Physiol.* 80:353–375.

Spray, D. C., and J. M. Burt. 1990. Structure-activity relations of the cardiac gap junction channel. *Am. J. Physiol.* 258:C195–C205.

Tabb, T., G. Thilander, A. Grover, E. Hertzberg, and R. Garfield. 1992. An immunochemical and immunocytologic study of the increase in myometrial gap junctions (and connexin 43) in rats and humans during pregnancy. *Am. J. Obstet. Gynecol.* 167:559–567.

Veenstra, R. D. 1990. Voltage-dependent gating of gap junction channels in embryonic chick ventricular cell pairs. *Am. J. Physiol.* 258: C662–C672.

Veenstra, R. D., H. Z. Wang, E. M. Westphale, and E. C. Beyer. 1992. Multiple connexins confer distinct regulatory and conductance properties of gap junctions in developing heart. *Circ. Res.* 71:1277–1283.

Wang, H. Z., J. Li, L. F. Lemanski, and R. D. Veenstra. 1992. Gating of mammalian cardiac gap junction channels by transjunctional voltage. *Biophys. J.* 63:139–151.

Weingart, R., and P. Maurer. 1988. Action potential transfer in cell pairs isolated from adult rat and guinea pig ventricles. *Circ. Res.* 63:72–80.

White, R. L., D. C. Spray, A. C. Campos de Carvalho, B. A. Wittenberg, and M. V. Bennett. 1985. Some electrical and pharmacological properties of gap junctions between adult ventricular myocytes. *Am. J. Physiol.* 249:C447–C455.

Wilders, R., and H. J. Jongsma. 1992. Limitations of the dual voltage clamp method in assaying conductance and kinetics of gap junction channels. *Biophys. J.* 63:942–953.